

Novel optical property of Ag@PPy nanoparticles

Sunjie Ye, Shujun Chen, Hongjuan Wang and Yun Lu

Department of Polymer Science and Engineering, State Key Laboratory of Coordination Chemistry,
School of Chemistry and Chemical Engineering, Nanjing University,
Nanjing 210093, P. R. China, E-mail: yunlu@nju.edu.cn

ABSTRACT

We characterized the novel luminescent properties of Ag@PPy (polypyrrole) nanoparticles, provided an explanation for the observed spectral shift in terms of the energy levels and exploited the Ag@PPy nanoparticles with doping-dependent emission peak shift as a fast reversible pH sensor. In our experiment, two peaks around 460nm and 520nm are observed in the emission spectra for Ag@PPy nanoparticles. These peaks blue-shift with the changed doping level of the PPy shell, which can be elucidated by consideration of the energy levels of Ag and PPy. The intensity of the two peaks alters with changing the volume ratio of the Ag core to the PPy shell, indicating that they are assigned to the $S_1 \rightarrow S_0$ transition of the PPy as well as Ag plasmon emission and the energy transfer between Ag and PPy, respectively. In addition, the peak position showed a reversible and fast response to the changed pH value of the medium, suggesting the potential applications of Ag@PPy nanoparticles as a reversible pH-sensor.

Keywords: Ag@PPy nanoparticle, luminescent property, emission spectra, pH-responsive, energy transfer.

1 INTRODUCTION

Composites of conducting polymers and metal nanoparticles can combine the advantages of both components, yielding materials with great academic and industrial interest[1,2]. The study of optical properties of nanocomposites is very important to gain a better understanding of their fundamental properties as well as exploit their potential new capability and function for applications. The difference in optical properties between composite materials and their constituent components depends largely on the chemical nature of each component as well as how the two or more components interact with each other[3]. The conjugated polymers with extended π -bonding, whose energy levels are often close to those of inorganic metals, can behave like organic semiconductors, making it more likely to mix their energy levels[4]. Therefore the interaction between the conjugated polymer and the metal is strong and can result in significant change

in optical properties of the composites compared to their isolated components.

In this work, we investigated the emission properties for Ag@PPy nanoparticles from the aspects of both fundamental mechanism and potential application based on the obtained experimental results. The significance of our work is not only in providing a route to adjust the emission properties of metal-conducting polymer nanocomposites by the doping effects, but also in paving the path for the metal-conducting polymer nanocomposites to be exploited as pH-sensors.

2 EXPERIMENTAL

The monomer pyrrole and oxidizer FeCl_3 with a proper ratio were added orderly to the beforehand prepared Ag colloid under vigorous magnetic stirring and reacted sequentially for 24h at room temperature to synthesize the Ag@PPy core/shell nanoparticles. Changing the amount of pyrrole and FeCl_3 can obtain the Ag@PPy nanoparticles with different volume ratios of the Ag colloid to the polypyrrole shell, and also with different doping levels for polypyrrole shell. The synthesized Ag colloids and the formed Ag@PPy nanoparticles were separated and dispersed in sequence with distilled water and ethanol by several centrifugation/dispersion cycles respectively, and dried under vacuum for 4h. All samples were dispersed in aqueous solutions for the spectral measurements.

3 RESULTS AND DISCUSSION

The TEM image indicated that the synthesized Ag@PPy nanoparticles have uniform sphere shape and core/shell structure without agglomeration (see Fig.1). Under different reaction conditions, the formed composite nanoparticles showed different core size or shell thickness.

For the as-prepared Ag@PPy nanoparticles, a special enhancement of peak at 1384 cm^{-1} corresponding to C-H bending vibration can be observed in their IR spectra (see Fig.2), indicating that the interaction between Ag and PPy at the interface may occur via $=\text{C}-\text{H}$. The increased doping level of shell PPy, leading to optimal energy matching between the Fermi levels of the Ag nanoparticles and the energy levels in the shell PPy molecules, could

enhance the surface-enhanced infrared absorption signal, which suggested that the mechanism of the enhancement might be a result of charge transfer.

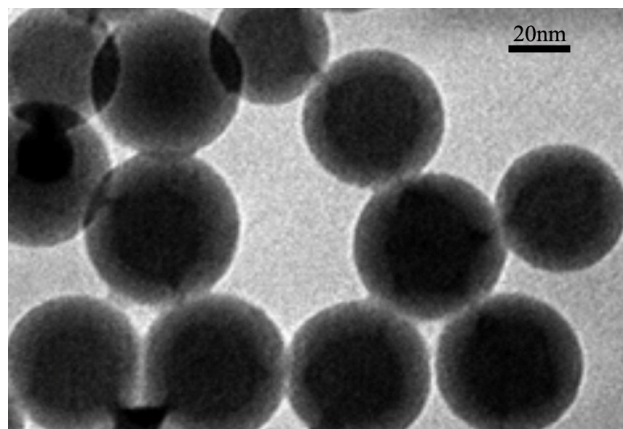


Fig.1 TEM images of the Ag@PPy core/shell nanoparticles

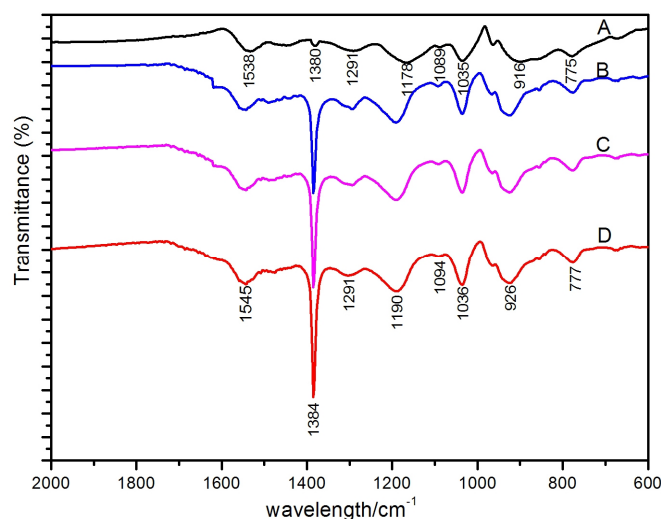


Fig.2 FTIR spectra of (A) pure PPy; (B) to (D) Ag@PPy nanoparticles with the increased doping level for shell PPy

Surface-enhanced Raman scattering (SERS) spectra of Ag@polypyrrole (PPy) nanoparticles with both 488 and 1064 nm excitation also were investigated. Experimental results as well as theoretical analysis demonstrated that electromagnetic (EM) enhancement and charge transfer (CT) both rebounded to the SERS effect of Ag@PPy nanoparticles. When near-IR excitation (1064 nm) was used for the SERS measurements, the contribution from CT was amplified relative to that from EM because the energy of the near-IR excitation is far from the surface plasmon resonance of the nanosized Ag particles. The increased doping level of PPy shell, leading to optimal energy matching between the Fermi levels of the Ag nanoparticles and the energy levels in PPy molecules, could obviously enhance the SERS signal.

The emission spectra of pure PPy (Fig.3D), Ag nanoparticles (Fig.3E) and Ag@PPy nanoparticles with

different volume ratios of Ag core to the PPy shell (Fig.3A to 3C) were shown in Fig.3. It can be seen that the spectrum for pure PPy displayed a peak at 455nm associated with $S_1 \rightarrow S_0$ transition between the LOMO and HOMO of PPy molecules[5,6]. Meanwhile, for Ag nanoparticles, its spectrum exhibited no obvious peak. In the case of the Ag@PPy nanoparticles with different volume ratios of Ag core and PPy shell, a shoulder peak located around 470nm whose intensity is enhanced with the increases of the volume ratio of PPy to Ag, could be attributed to the $S_1 \rightarrow S_0$ transition in PPy shell. In addition, a new peak centered around 520nm appeared, which strengthens with the increased volume ratio of Ag to PPy. We ascribed the peak around 520nm to the interaction between the Ag core and PPy shell and also the contributes of charge transfer.

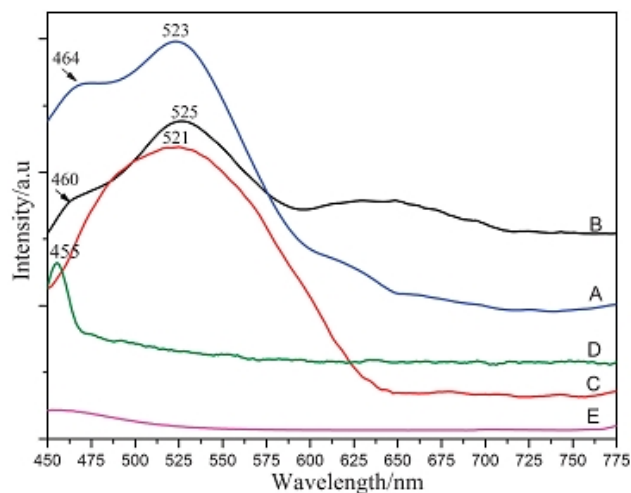


Fig.3 The emission spectra of Ag@PPy nanoparticles with different vilume ratios of the Ag core to the PPy shell

The charge transfer could be described as the following two processes: 1) The electron transfer from Ag Fermi level to the additional π^* orbit of PPy. Due to the interaction between the Ag core and PPy shell, the doped Cl^- ion could create a new dipole at the interface of Ag@PPy nanoparcle, consequently increase the Fermi level of Ag, making it closer to the additional π^* orbit. As a result, the electrons are prompted to transfer between Ag Fermi level and the additional π^* orbit. Equilibrium is reached when the two energy levels are equal[7]. However, this process does not contribute directly to the emission signal, merely endowing Ag Fermi level to act as an electronic state that can trap the electron within the PPy bandgap. 2) The electron relaxation within the PPy bandgap via the trapping of electron by Ag Fermi level. The bandgap photoexcitaiton of the PPy produces an electron in the LUMO and a hole in the HOMO, forming a nonequilibrium state. To achieve the equilibrium, the photogenerated electron is subject to be relaxed to the HOMO and recombined with the hole[3]. During its relaxation, the electron is trapped by the Fermi level of Ag and then relaxed to the PPy HOMO, emitting the photon, that is, the observed emission signal of the Ag@PPy nanoparticles.

Figure 4 showed the emission spectra of Ag@PPy nanoparticles with different doping levels. It can be seen that, the two emission peaks for Ag@PPy nanoparticles shift to shorter wavelength (higher energy) with the increasing doping level of Cl⁻ ions, suggesting that the doping can alter the emission properties of the Ag@PPy nanoparticles, which could also be interpreted from the change of the energy levels of Ag and PPy due to the doping effect. Accompanying with the generation of additional orbit caused by doping, the HOMO and LUMO for PPy are relocated because of the perturbation caused by new orbits. Eventually, the HOMO for PPy is lowered and the LUMO is raised. The energy gap between the HOMO and LUMO, or the HOMO and the Fermi level for Ag is enlarged. The higher doping level leads to the larger energy gap, resulting in the blue shift of corresponding emission peak, in agreement with what we have observed.

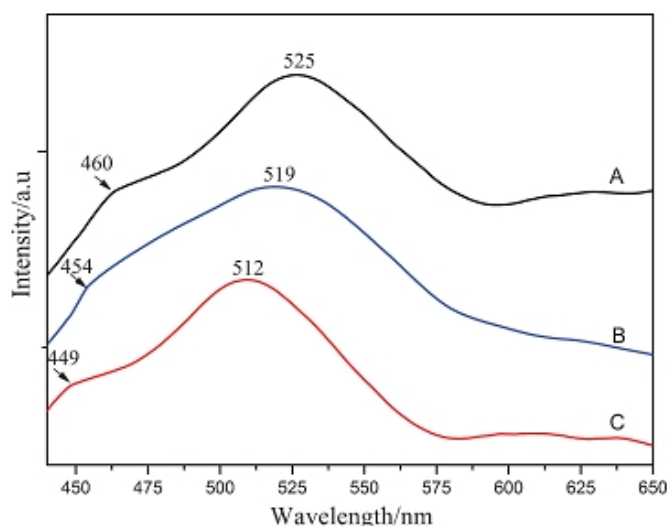


Fig.4 The emission spectra of Ag@PPy nanoparticles with different doping level.

Depending on the above results and the fact that the doping level of conducting polymer is sensitive to the acidity or alkalinity of the medium[8], we record the emission spectra of Ag@PPy nanoparticles in aqueous solutions with different pH values (shown in Figure 5) to explore the potential pH-sensing function for Ag@PPy nanoparticles. With the increased pH value of the aqueous solution, the peak dramatically shifts to longer wavelength. It is generally considered that, for PPy, acid environment causes doping, whereas alkali cancels the doping, that is, the Ag@PPy nanoparticles dispersed in the aqueous solutions with larger pH value possess lower doping level, thus show the red-shifted peak in the emission spectra. The sensitivity of the emission peak position to the pH value of the environment endows the Ag@PPy nanoparticles the potential pH-sensing function.

The easy and reversible switching behavior of PPy between doping and undoping [9] further provides the possibility for Ag@PPy nanoparticles to be exploited as

reversible pH-sensor. For the profound investigation of the pH-sensing function of the Ag@PPy nanoparticles, we measure the emission spectra for Ag@PPy nanoparticles during the gradual alkalization and reverse acidification of the aqueous solutions. For the Ag@PPy nanoparticles dispersed in the aqueous solutions with initial pH value of 1.4, the emission peak appears at 500nm (Figure 6aA). The subsequent addition of aqueous NaOH solution adjusts the pH value progressively from 1.4 to 8.9, accompanied by the emission peak shift from 500nm to 545nm (Figure 6a B-E). Afterwards, with the addition of conc. HCl lowering the pH value in steps from 8.9 to 1.5, the emission peak blue shifts from 545nm to 505nm (Figure 6b A-D). These results revealed that the emission peak position for Ag@PPy nanoparticles is a reversible response to the pH value of the medium.

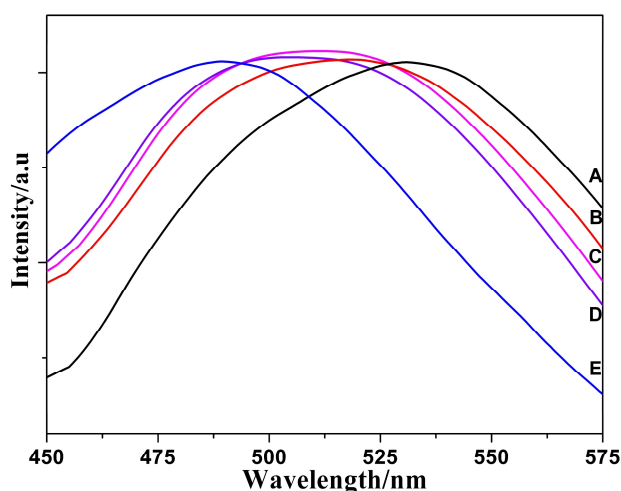


Fig.5 The emission spectra ($\lambda_{\text{ex}}=420\text{nm}$) of Ag@PPy nanoparticles dispersed in aqueous solutions with different pH values (A) pH=9.2; (B) pH=7.4; (C) pH=4.5; (D) pH=3.4; (E) pH=1.0

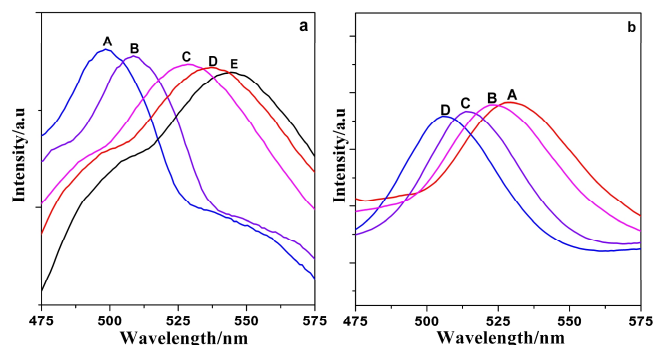


Fig.6 (a) Emission spectra of Ag@PPy nanoparticles in aqueous solutions at pH values of (A) 1.4, (B) 3.3, (C) 5.5, (D) 7.8, (E) 8.9 adjusted by the sequential additions of aqueous NaOH solutions. (b) Emission spectra of Ag@PPy nanoparticles in aqueous solutions at pH values of (A) 7.7, (B) 5.3, (C) 3.5, (D) 1.5 adjusted by the sequential additions of conc. HCl.

During the gradual alkalization and acidification process, after each adjustment of the pH value, the data read from the pH-meter reach a steady value within ca. 3 seconds (the response time of the pH-meter included), and the emission spectra for each sample are recorded within 3.75 seconds (scan from 450nm to 600nm, scan rate 2400nm/min), indicating a fast response process. These behaviors revealed that the shift of emission peak position for Ag@PPy nanoparticles is a reversible and rapid response to the pH value of the medium, demonstrating the potential applications of Ag@PPy nanoparticles as a reversible pH-sensor.

REFERENCES

- [1] G. Sonmez, Chem. Commun. 5251, 2005.
- [2] G. G. Wallace, G. M. Spinks, L. A. P. Kane-Maquire, P. R. Teasdale, Conductive Electroactive Polymers: Intelligent Materials Systems, 2nded., CRC Press, Boca Raton, Florida, USA, 2003.

- [3] J. Z. Zhang, Optical Properties and Spectroscopy of Nanomaterials, World Scientific Publishing Co. Pte. Ltd, 2009.
- [4] E. Holder, N. Tessler and A.L. Rogach, J. Mater. Chem. 1064, 18, 2008.
- [5] B. Liu and G. C. Bazan, J. Am. Chem. Soc., 128, 1188, 2006.
- [6] C. M. Che, C. W. Wan, Chem. Commun., 721, 2001.
- [7] S. J. Ye, L. Fang, Y. Lu, J. Raman Spectrosc., 41, 1119, 2010.
- [8] C. A. Cutler, M. Bouguettaya, T. S. Kang J. R. Reynolds, Macromolecules, 38, 3068, 2005.
- [9] T. A. Skotheim, John. R. Reynolds, Handbook of Conduction Polymers 3rd edition, CRC Press, 2007.

ACKNOWLEDGEMENTS

This work was supported by the National Natural Science Foundation of China (No.20974043 and No.50773030).